Desalination and Water Treatment
www.deswater.com
doi: 10.1080/19443994.2013.809984

52 (2014) 4935–4941
July

Taylor & Francis
Taylor & Francis Group

Adsorption of nitrate ions onto activated carbon prepared from rice husk by NaOH activation

Ying Zhang[a], Xiao-Lan Song[a,*], Shu-Tao Huang[a], Bai-Yang Geng[a], Chi-Hsien Chang[b], I-Yen Sung[b]

[a]*Department of Inorganic Materials, School of Mineral Processing and Bioengineering, Central South University, 932 Lushan Road South, Changsha Hunan 410083, P.R. China*
Tel. +86 13808422020; Fax: +86 0731 88710804; email: xlsong365@126.com
[b]*Component Engineering, Test and Verification Center, Askey Technology (Jiangsu) Ltd., Suzhou Jiangsu 215200, P.R. China*

Received 30 June 2012; Accepted 6 May 2013

ABSTRACT

Precursor was prepared from rice husk under different carbonization temperatures. Then, activated carbon (AC) was synthesized by NaOH activation. The specific surface area of carbon increased with temperature rise up to 600°C, but decreased rapidly over 600°C. So, the AC obtained at 600°C possessed the outstanding surface area of 2,802 m^2/g. And, its adsorption activity of nitrate was carried out at initial concentration of 50–400 mg/L. The results showed that the maximum adsorption capacity and removal percentage of NO_3^- were 70.2 mg/g and 70.6%, respectively. Besides, the experimental data were evaluated by Langmuir, Freundlich, and Redlich–Peterson isotherms. In kinetic studies, it was observed that the results were well explained by the pseudo second-order model. In addition, the Gibbs free energy change of −17.0 kJ/mol indicated that the adsorption process was spontaneous.

Keywords: Activated carbon; Rice husk; Nitrate; Adsorption

1. Introduction

Nowadays, industrial and agricultural productions have generated large amounts of pollutants such as organic compounds, inorganic anions, and heavy metals. Among them, nitrate (NO_3^-) could change into the carcinogenic nitrite (NO_2^-), increasing the risk of cancer for humans [1]. Thus, there are some methods to remove NO_3^- [1,2], including chemical denitrification, ion exchange, reverse osmosis, adsorption, and biological treatment. Of these, adsorption with activated carbon (AC) is a convenient and efficient technology.

As a porous material, AC is widely used in water treatment. Due to the wide availability, the date pit [3], coconut [4], bamboo [5], wood [6], and other wastes have been used as raw materials of ACs, recently. Further, China is the largest rice producer with annual output of 200 million tons. So rice husk is an ideal choice for preparing AC [7–11]. However, the specific surface area of AC was usually low because the high ash content (silica) in rice husk obstructed the pore development [12]. But, traditional activators like H_3PO_4 or $ZnCl_2$ [13] cannot remove SiO_2. Kalderis et al. [7] and Teker et al. [10] reported that AC prepared from rice husk by $ZnCl_2$ activation exhibited

*Corresponding author.

the surface area of 811 and 319 m^2/g. Taking into account the reaction, NaOH was selected as the activator ($2NaOH + SiO_2 \rightarrow Na_2SiO_3 + H_2O$). The solid NaOH was mixed directly with the precursor for activation, without solution impregnation in the previous works [13,14]. The reaction mechanism was $6NaOH + 2C \rightarrow 2Na + 2Na_2CO_3 + 3H_2$ [14].

In general, the production of AC included carbonization and activation, and preparation conditions showed significant influences on the properties of ACs [13]. Although there were many reports on the reaction parameters such as activation temperature or activator ratio [2,7,8], very few studies have been focused on the carbonization process. Moreover, there are only a few studies about the adsorption for NO_3^- onto ACs [1].

The objective of the present work is to prepare ACs with high specific surface area from rice husk by NaOH and to investigate its adsorption performance for the nitrate. So batch adsorption experiments had been carried out at room temperature. The experimental data had been estimated by three adsorption isotherms. Furthermore, kinetic and thermodynamic studies were also undertaken.

2. Experimental

2.1. Preparation of activated carbons

Rice husk was obtained from Changsha. Its ash and fixed carbon contents were 12.5 and 22.5 wt.%, respectively. Chemical reagents were all of analytical grade.

Firstly, the rice husk was carbonized under N_2 atmosphere at 500, 600, or 700°C for 2 h. Then, the solid NaOH was mixed with the carbonized rice husk at mass ratio for the NaOH/precursor of three [14]. Subsequently, reactants were heated up to 800°C for 2 h. At last, the product was washed and dried. Additionally, the samples carbonized at 500, 600, and 700°C were labeled as AC500, AC600, and AC700.

2.2. Characterizations of activated carbons

Thermal analysis was investigated by a thermo gravimetric–derivative thermo gravimetric (TG–DTG) analyzer (STA449c, NETZSCH). Rice husk was heated at a rate of 10°C/min from room temperature up to 1,000°C in argon atmosphere.

Specific surface area (S_a) was obtained by the Brunauer–Emmett–Teller (BET) method using N_2 adsorption data at 77 K with a gas sorption analyzer (Autosorb-1, Quantachrome). The pore size distribution was estimated using the density functional theory (DFT) [15]. Total pore volume (V_t) was calculated at relative pressure $P/P_0 = 0.99$ and the average pore diameter (d_a) was evaluated by: $d_a = 2000V_t/S_a$. Besides, the Dubinin–Radushkevich (DR) model was used to evaluate micropore surface area (S_m) and volume (V_m) [16].

Microstructure was examined by using a FEI Quantn-200 scanning electron microscopy (SEM) with the accelerated voltage of 20 kV.

Ash content was determined by heating the sample at 600°C for 2 h until the weight remained constant.

2.3. Adsorption of nitrate

KNO_3 was used as the adsorbate and the concentration of NO_3^- was determined by an ultraviolet spectrophotometer (SP-756P, Spectrum) at a wavelength of 220 nm. Absorbance values were determined with a series of known concentrations to depict the concentration-absorbance line. In adsorption tests, 0.2 g of AC was added into 100 mL of NO_3^- solution (50, 100, 200, 300, and 400 mg/L) at 20°C. The adsorption capacity q_e (mg/g) and removal percentage of NO_3^- (%) were calculated by the following equations:

$$q_e = \frac{(C_0 - C_e) \cdot V}{M} \quad (1)$$

$$\text{Removal } (\%) = \frac{C_0 - C_e}{C_0} \quad (2)$$

where C_0 and C_e are initial and equilibrium NO_3^- concentrations (mg/L), respectively; V is volume of solution (L) and M is mass of AC (g).

3. Results and discussion

3.1. Properties of activated carbons

Fig. 1 shows the TG–DTG curves of rice husk. Evaporation of water took place at temperatures ranging from 30 to 150°C. In the DTG curve, a significant weight loss peak between 150 and 500°C was ascribed to the pyrolysis of abundant celluloses [17]. Above 500°C, the reaction was nearly completed and the residue was just carbon and ash (silica). The main purpose of carbonization was to remove moisture and volatile organic compounds. Thus, the carbonization temperature was selected from 500 to 700°C.

The adsorption–desorption isotherms of N_2 and DFT pore size distributions for ACs are presented in Fig. 2(a) and (b). And, the pore texture parameters are

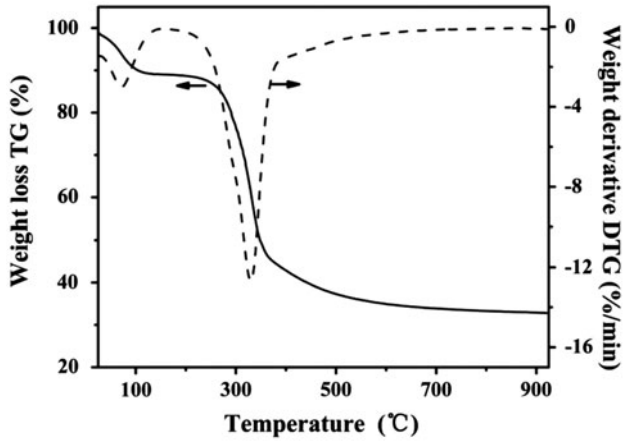

Fig. 1. TG–DTG curves of rice husk.

listed in Table 1. It could be seen that three samples exhibited type I isotherms corresponding to micropores. Meanwhile, they all displayed a hysteresis loop of type H4 for narrow slit-like mesopores [18]. Since high carbonization temperature accelerated the pyrolysis of material to form pore structure [19], the sample of AC600 presented greater adsorption volume of N_2 compared with AC500. And, its larger hysteresis loop indicated the further development of mesopores. But, the isotherm of AC700 changed considerably, with minor N_2 adsorption volume and larger hysteresis loop. One possible reason was that numerous micropores combined into mesopores at 700℃ [19], as shown in Fig. 2(b). Moreover, the S_a increased according to the following order: AC600 > AC500 > AC700, and this complied with the above discussion. As a result, the AC600 was microporous with the maximum S_a of 2,802 m^2/g and then it was used for adsorption experiments.

The morphology of AC600 is elucidated in Fig. 3. It was found that the sample showed irregular shape with fragmentary structure of particles, exhibiting the pyrolysis of material during preparation [12]. And, micrograph images showed that the carbon presented a porous structure with some macropores and mesopores randomly distributed on the surface.

As can be seen from Table 1, the ash contents of ACs were all less than the high value of 12.5 wt.% in rice husk. During the preparation, NaOH reacted with SiO_2 to open the blocking pore structure, leaving the low ash carbon skeleton [12]. It indicated that NaOH could effectively remove ash and improve the surface area of carbon.

Table 2 provides a summary of the activation condition and surface area S_a of AC for this study and other researches. It was found that compared with the AC sample prepared by $ZnCl_2$, the AC obtained by NaOH activation showed the low ash content due to the reaction between NaOH and SiO_2 [12,13]. In this case, the sample exhibited an excellent S_a of 2,802 m^2/g. According to these results, the preparation process in this study was an effective method to obtain ACs with high S_a and low ash content.

3.2. Adsorption equilibrium

Fig. 4 exhibits the adsorption capacities and removal percentages of NO_3^- on AC600. Adsorption capacities were found to increase as concentrations of NO_3^- increase from 50 to 400 mg/L. The adsorption capacity of NO_3^- was only 17.7 mg/g for 50 mg/L of NO_3^- solution. And, the maximum adsorption amount, up to 70.2 mg/g, was obtained by adsorbing 400 mg/L of NO_3^-. In addition, the maximum removal percentage for NO_3^- (70.6%) was gained for the concentration

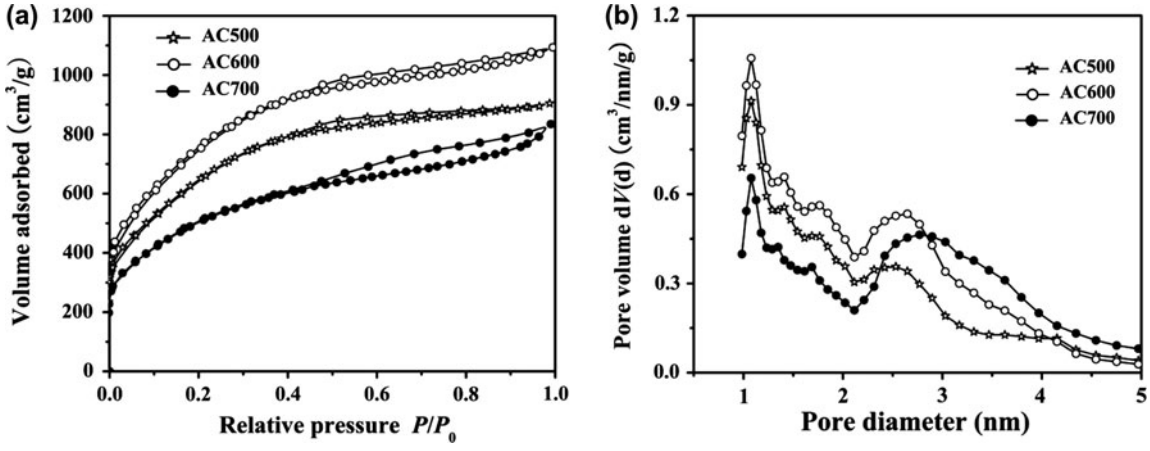

Fig. 2. Adsorption–desorption isotherms of N_2 (a) and DFT pore size distribution (b) for ACs.

Table 1
Porous properties and ash contents of ACs under different carbonization temperatures

Samples	AC500	AC600	AC700
S_a (m^2/g)	2,526	2,802	1,857
S_m (m^2/g)	2,152	2,373	1,242
V_t (cm^3/g)	1.517	1.690	1.389
V_m (cm^3/g)	0.765	0.843	0.432
d_a (nm)	1.20	1.21	1.50
Ash (wt.%)	3.94	3.52	3.23

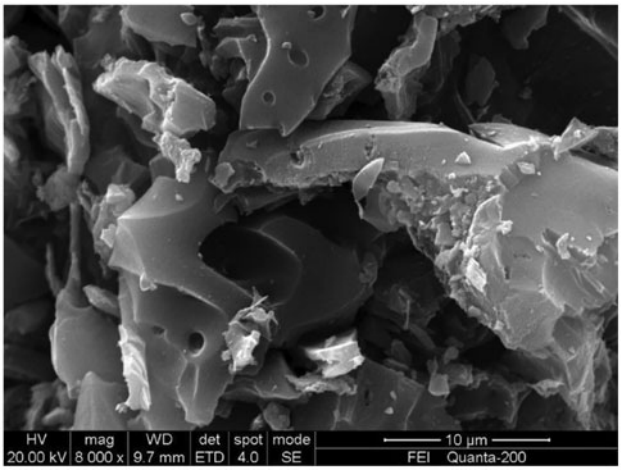

Fig. 3. SEM image of surface for AC600.

of 50 mg/L. Under certain amount of AC, the higher concentration of NO_3^- led the larger adsorption capacity. On the other hand, the remaining concentration of NO_3^- in solution was also higher, naturally giving the low removal percentage [20].

Langmuir and Freundlich isotherms were generally used to describe the adsorption process. Besides, the Redlich–Peterson isotherm was an empirical

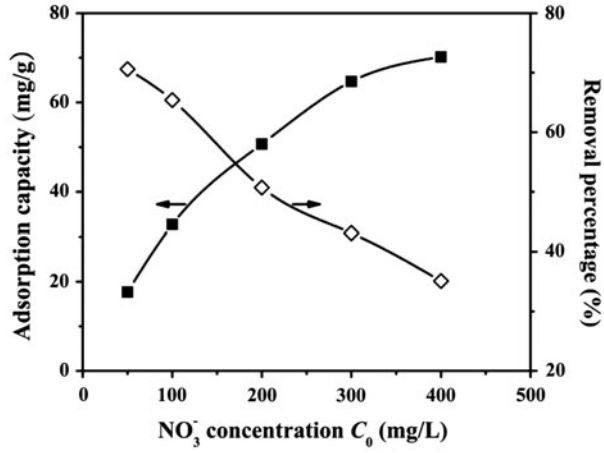

Fig. 4. Adsorption capacities and removal percentages of NO_3^- on ACs.

model between them. The Langmuir (3), Freundlich (4) and Redlich–Peterson (5) equations were given as follows [21,22]:

$$q_e = \frac{q_m \cdot K_L \cdot C_e}{1 + K_L \cdot C_e} \quad (3)$$

$$q_e = K_F \cdot C_e^{\frac{1}{n}} \quad (4)$$

$$q_e = \frac{K_{RP} \cdot C_e}{1 + \alpha \cdot C_e^{\beta}} \quad (5)$$

where q_m (mg/g) is maximum monolayer adsorption capacity, K_L (L/mg) is Langmuir isotherm parameter; K_F is Freundlich constant $(mg/g)(mg/L)^n$, and n is dimensionless heterogeneity factor; K_{RP} (L/g) and α $(L/mg)^{\beta}$ are Redlich–Peterson constants, and β is the exponent which lies between 0 and 1 (Langmuir form) [22]. In addition, the correlation coefficient (R^2) was evaluated by plotting the graph for models.

Table 2
Summary for S_a of ACs from various raw materials under optimal activation condition

Raw material	Activator	Mass ratio	S_a (m^2/g)	Ash (wt.%)	Reference
Rice husk	NaOH	3	2,802	3.52	This work
Rice husk	$ZnCl_2$	1	811	27.8	[7]
Rice husk	$ZnCl_2$	0.022	319	25.35	[10]
Rice husk	H_3PO_4	–	451.82	–	[8]
Sugar beet bagasse	$ZnCl_2$	3	1826	–	[2]
Bamboo	K_2CO_3	2	2,175	–	[5]
Fir sawdust	$ZnCl_2$	1	1,079	–	[6]

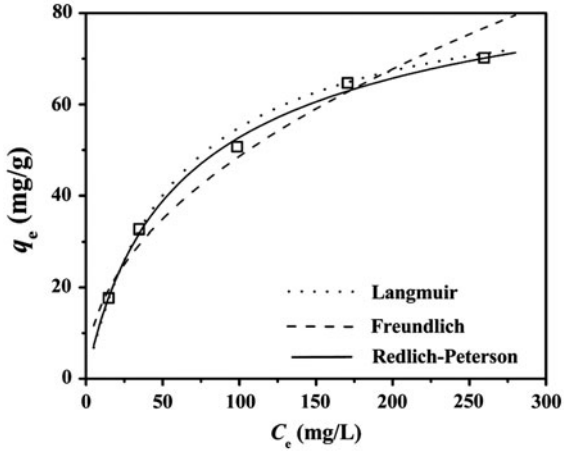

Fig. 5. Langmuir, Freundlich and Redlich–Peterson isotherms of NO_3^- adsorption.

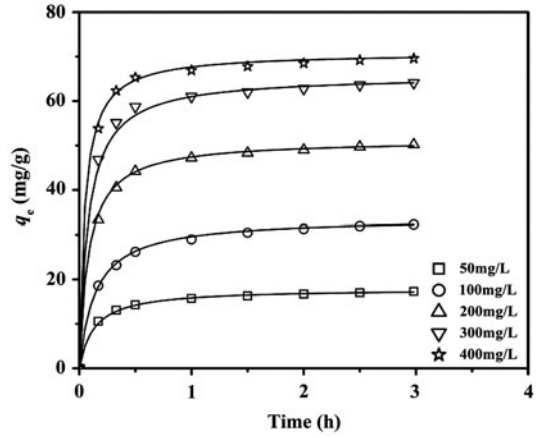

Fig. 6. Pseudo second-order kinetic model plots for NO_3^- adsorption on ACs.

Fig. 5 exhibits the plots of three isotherms for NO_3^- adsorption onto ACs. The parameters of three isotherms are given in Table 3. For the Langmuir model, the monolayer adsorption capacity q_m was found to be 86.2 mg/g. On the other hand, the favorable characteristics of Freundlich model were noted because of the higher value of n (2.09) and K_F (5.38). Meanwhile, β in Redlich–Peterson equation was 0.918 (close to 1). In summary, both of Langmuir and Redlich–Peterson isotherms were greatly suitable to explicate experimental data due to R^2 of 0.992 and 0.998. Therefore, the adsorption of NO_3^- onto ACs was hybrid with a main component being monolayer adsorption [21,22].

3.3. Adsorption kinetics

In kinetic study, the Lagergren model was used to examine the adsorption. The pseudo first-order (6) and second-order (7) equations were given as follows [23–25]:

$$q_t = q_e(1 - e^{-K_1 \cdot t}) \tag{6}$$

$$q_t = \frac{q_e^2 \cdot K_2 \cdot t}{1 + q_e \cdot K_2 \cdot t} \tag{7}$$

where q_t is the adsorbed quantity of NO_3^- at time (mg/g), K_1 is rate constant of pseudo first-order sorption (h^{-1}), t is adsorption time (h), and K_2 is rate constant of pseudo second-order sorption (g/(mg h)).

Table 4
Parameters of adsorption kinetics on activated carbons in NO_3^- solution

Concentration (mg/L)	Pseudo first-order model			Pseudo second-order model		
	q_e (mg/g)	K_1 (h^{-1})	R^2	q_e (mg/g)	K_2 (g/(mg h))	R^2
50	6.2	0.92	0.964	17.9	0.43	1.000
100	13.7	1.17	0.979	33.8	0.21	1.000
200	14.3	1.12	0.956	51.3	0.24	1.000
300	13.7	1.04	0.946	65.8	0.19	1.000
400	11.5	1.00	0.931	70.9	0.29	1.000

Table 3
Coefficients of isotherm models for NO_3^- adsorption

Isotherms	Parameters			R^2
Langmuir	K_L (L/mg) 0.017	q_m (mg/g) 86.2		0.992
Freundlich	K_F (mg/g)(mg/L)^n 5.38	n 2.09		0.964
Redlich–Peterson	K_{PR} (L/g) 1.656	α (L/mg)$^\beta$ 0.031	β 0.918	0.998

The kinetic model plots for NO_3^- adsorption, with time, are shown in Fig. 6 and the equation parameters are given in Table 4. It showed that the adsorption capacities of NO_3^- increased rapidly during the initial 30 min and became almost constant after 1 h. With the prolongation of time, most of the adsorption sites had been occupied thus limiting free sites for NO_3^- ion to attach on [26].

On the other hand, the obtained values of q_e and R^2 from the pseudo first-order model were not appropriate to describe the kinetics for NO_3^- adsorption. On the contrary, the calculated values of q_e for the pseudo second-order model agreed with experiment data. Furthermore, the R^2 were in between 0.99 and 1 for pseudo second-order model. Thus, the adsorption data were well correlated by the pseudo second-order model [2,20]. This fact suggested that the adsorption rate for AC was dependent on the availability of adsorption sites rather than the NO_3^- concentration in solution [23]. Additionally, the adsorption curves were single and smooth, indicating the monolayer adsorption of NO_3^- [23]. Such a finding was in good agreement with the Redlich–Peterson isotherm.

3.4. Adsorption thermodynamics

The thermodynamics was studied to gain an insight into the temperature behaviors. The famous parameter of Gibbs free energy change ($\triangle G^\circ$, kJ/mol) was determined according to the following equation [21]:

$$\Delta G^\circ = -R \cdot T \cdot \ln K \quad (8)$$

where K is from K_L in Langmuir equation (L/mol), R is the gas constant (8.314 J/mol K), and T is the temperature in Kelvin (K).

In this study, K was obtained as 1,054 L/mol from K_L (0.017 L/mg) at T of 293 K. Thereby, negative $\triangle G^\circ$ of −17.0 kJ/mol was calculated, revealing the spontaneous nature of adsorption. In general, the $\triangle G^\circ$ values were in the range from 0 to −20 kJ/mol and −80 to −400 kJ/mol for physical and chemical adsorptions, respectively [21]. Therefore, the $\triangle G^\circ$ value was in the range from 0 to −20 kJ/mol, indicating that the adsorption was mainly physical in nature.

Generally, the adsorption activity was closely related to the specific surface area and pore size distribution of ACs. The sample of AC600 exhibited a high surface area, S_a, of 2,802 m^2/g. Besides, it was microporous with large S_m of 2,373 m^2/g and V_m of 0.843 cm^3/g. In this case, nitrate ions could be easily diffused into micropores [22,23], exhibiting the higher NO_3^- adsorption capacity of 70.2 mg/g than values of 26 [20] and 27.55 mg/g [2] reported in literatures. Hence, microporous ACs prepared in this study were very suitable for small molecule adsorption, like NO_3^-.

4. Conclusions

In the present work, ACs prepared from rice husk with NaOH were used for adsorption of nitrate at 20°C. The surface area was closely related to the carbonization temperature. As a result, the sample carbonizing at 600°C presented the optimum S_a of 2,802 m^2/g. Since it has numerous micropores, NO_3^- could be easily diffused into the pores of AC. At initial NO_3^- concentration of 400 mg/L, the maximum adsorption capacity was recorded at 70.2 mg/g. On the contrary, the maximum removal percentage up to 70.6% at concentration of 50 mg/L. Additionally, the experimental data were well explained by the Langmuir, Redlich–Peterson, and pseudo second-order models, implying the major monolayer adsorption. In addition, the $\triangle G^\circ$ value of −17.0 kJ/mol was obtained, indicating the spontaneous nature of adsorption process. Therefore, the results showed that the rice husk was a good candidate for microporous carbon production. And, favorable removal of NO_3^- exhibited that the AC could be considered as the low cost and efficient adsorbent for sewage treatment.

Symbols

q_e — adsorption capacity, mg/g
C_0 — initial concentration of NO_3^-, mg/L
C_e — equilibrium concentration of NO_3^-, mg/L
V — volume of solution, L
M — mass of AC, g
q_m — monolayer adsorption capacity from Langmuir equation, mg/g
K_L — Langmuir isotherm parameter, L/mg
K_F — Freundlich isotherm parameter, (mg/g)(mg/L)^n
n — dimensionless heterogeneity factor in Freundlich equation
K_{RP} — Redlich–Peterson isotherm parameter, L/g
α — Redlich–Peterson isotherm parameter, (L/mg)$^\beta$
β — exponent in Redlich–Peterson equation
q_t — adsorbed capacity of NO_3^- at time, mg/g
t — adsorption time, h
K_1 — rate constant of pseudo first-order sorption, h^{-1}
K_2 — rate constant of pseudo second-order sorption, g/(mg h)
K — adsorption equilibrium constant
R — gas constant, J/mol K
T — temperature in Kelvin, K
S_a — specific surface area of AC, m^2/g

V_t — total pore volume of AC, cm^3/g
d_a — average pore diameter, nm
S_m — specific surface area of micropore, m^2/g
V_m — pore volume of micropore, cm^3/g

Acknowledgments

This research was supported by the projects of International Cooperation of Science and Technology Ministry of China (No. 2005DFBA028). The authors acknowledge Mr. Chen Hao and Mrs. Zhou Jing, Component Engineering, Askey Technology (Jiangsu). Ltd., China, who performed the correction for language.

References

[1] A. Bhatnagar, M. Sillanpää, A review of emerging adsorbents for nitrate removal from water, Chem. Eng. J. 168 (2011) 493–504.
[2] H. Demiral, G. Gündüzoğlu, Removal of nitrate from aqueous solutions by activated carbon prepared from sugar beet bagasse, Bioresour. Technol. 101 (2010) 1675–1680.
[3] N. Bouchemal, F. Addoun, Adsorption of dyes from aqueous solution onto activated carbons prepared from date pits: The effect of adsorbents pore size distribution, Desalin. Water Treat. 7 (2009) 242–250.
[4] X.L. Song, H.Y. Liu, L. Cheng, Y.X. Qu, Surface modification of coconut-based activated carbon by liquid-phase oxidation and its effects on lead ion adsorption, Desalination 255 (2010) 78–83.
[5] T. Horikawa, Y. Kitakaze, T. Sekida, J. Hayashi, M. Katoh, Characteristics and humidity control capacity of activated carbon from bamboo, Bioresour. Technol. 101 (2010) 3964–3969.
[6] J. Yang, K.Q. Qiu, Preparation of activated carbon by chemical activation under vacuum, Environ. Sci. Technol. 43 (2009) 3385–3390.
[7] D. Kalderis, D. Koutoulakis, P. Paraskeva, E. Diamadopoulos, E. Otal, J.O.D. Valle, C. Fernández-Pereira, Adsorption of polluting substances on activated carbons prepared from rice husk and sugarcane bagasse, Chem. Eng. J. 144 (2008) 42–50.
[8] N.S. Awwad, H.M.H. Gad, M.I. Ahmad, H.F. Aly, Sorption of lanthanum and erbium from aqueous solution by activated carbon prepared from rice husk, Colloid Surf. B 81 (2010) 593–599.
[9] A.A. Olanrewaju, A.O. Sarafadeen, I.A. Omotayo, Isothermal studies of adsorption of acenaphthene from aqueous solution onto activated carbon produced from rice (Oryza sativa) husk, Desalin. Water Treat. 46 (2012) 87–95.
[10] M. Teker, M. İmamoğlu, O. Saltabas, Adsorption of copper and cadmium ions by activated carbon from rice hulls, Turk. J. Chem. 23 (1999) 185–191.
[11] M. Teker, M. İmamoğlu, N. Bocek, Adsorption of some textile dyes on activated carbon prepared from rice hulls, Fresenius Environ. Bull. 18 (2009) 709–714.
[12] A.H. Basta, V. Fierro, H. El-Saied, A. Celzard, 2-Steps KOH activation of rice straw: An efficient method for preparing high-performance activated carbons, Bioresour. Technol. 100 (2009) 3941–3947.
[13] O. Ioannidou, A. Zabaniotou, Agricultural residues as precursors for activated carbon production–a review, Renew. Sust. Energy Rev. 11 (2007) 1966–2005.
[14] X.L. Song, Y. Zhang, C.M. Chang, Novel method for preparing activated carbons with high specific surface area from rice husk, Ind. Eng. Chem. Res. 51 (2012) 15075–15081.
[15] A.V. Neimark, Y.Z. Lin, P.I. Ravikovitch, M. Thommes, Quenched solid density functional theory and pore size analysis of micro–mesoporous carbons, Carbon 47 (2009) 1617–1628.
[16] C. Scherdel, G. Reichenauer, M. Wiener, Relationship between pore volumes and surface areas derived from the evaluation of N_2-sorption data by DR–BET- and t-plot, Micropor. Mesopor. Mater. 132 (2010) 572–575.
[17] K. Sun, J.C. Jiang, Preparation and characterization of activated carbon from rubber-seed shell by physical activation with steam, Biomass Bioenergy 34 (2010) 539–544.
[18] C. Sangwichien, G.L. Aranovich, M.D. Donohue, Density functional theory predictions of adsorption isotherms with hysteresis loops, Colloid Surf. A 206 (2002) 313–320.
[19] K. Mohanty, M. Jha, B.C. Meikap, M.N. Biswas, Preparation and characterization of activated carbons from Terminalia Arjuna nut with zinc chloride activation for the removal of phenol from wastewater, Ind. Eng. Chem. Res. 44 (2005) 4128–4138.
[20] D.W. Cho, C.M. Chon, Y. Kim, Y. Kim, B.H. Jeon, F.W. Schwartz, E.S. Lee, H. Song, Adsorption of nitrate and Cr(VI) by cationic polymer-modified granular activated carbon, Chem. Eng. J. 175 (2011) 298–305.
[21] Q.S. Liu, T. Zheng, P. Wang, J.P. Jiang, N. Li, Adsorption isotherm, kinetic and mechanism studies of some substituted phenols on activated carbon fibers, Chem. Eng. J. 157 (2010) 348–356.
[22] W. Plazinski, W. Rudzinski, Kinetics of adsorption at solid/solution interfaces controlled by intraparticle diffusion: A theoretical analysis, J. Phys. Chem. C 113 (2009) 12495–12501.
[23] M.U. Dural, L. Cavas, S.K. Papageorgiou, F.K. Katsaros, Methylene blue adsorption on activated carbon prepared from Posidonia oceanica (L.) dead leaves: Kinetics and equilibrium studies, Chem. Eng. J. 168 (2011) 77–85.
[24] S. Lagergren, About the theory of so-called adsorption of soluble substance, Kung Sven. Veten. Hand. 24 (1898) 1–39.
[25] Y.S. Ho, G. McKay, Kinetic models for the sorption of dye from aqueous solution by wood, J. Environ. Sci. Health Part B, Process. Safe Environ. Protect. 76 (1998) 183–191.
[26] Y. Matsui, N. Ando, H. Sasaki, T. Matsushita, K. Ohno, Branched pore kinetic model analysis of geosmin adsorption on super-powdered activated carbon, Water Res. 43 (2009) 3095–3103.